Organic N and P in eutrophic fjord sediments

Rates of mineralization and consequences for internal nutrient loading

Valdemarsen, Thomas Bruun; Quintana, Cintia Organo; Flindt, Mogens; Kristensen, Erik

Published in:
Biogeosciences

DOI:
10.5194/bg-12-1765-2015

Publication date:
2015

Document version
Publisher's PDF, also known as Version of record

Biogeosciences, 12, 1765–1779, 2015
www.biogeosciences.net/12/1765/2015/
doi:10.5194/bg-12-1765-2015

Biogeosciences Open Access

Organic N and P in eutrophic fjord sediments – rates of mineralization and consequences for internal nutrient loading

T. Valdemarsen[1], C. O. Quintana[1,2], M. R. Flindt[1], and E. Kristensen[1]

[1]Institute of Biology, University of Southern Denmark, Odensee, Denmark
[2]Instituto Oceanográfico, Universidade de São Paulo, São Paulo, Brazil

Correspondence to: T. Valdemarsen (valdemarsen@biology.sdu.dk)

Received: 8 August 2014 – Published in Biogeosciences Discuss.: 27 October 2014
Revised: 24 February 2015 – Accepted: 1 March 2015 – Published: 18 March 2015

Abstract. Nutrient release from the sediments in shallow eutrophic estuaries may counteract reductions of the external nutrient load and prevent or prolong ecosystem recovery. The magnitude and temporal dynamics of this potential source, termed internal nutrient loading, is poorly understood. We quantified the internal nutrient loading driven by microbial mineralization of accumulated organic N (ON) and P (OP) in sediments from a shallow eutrophic estuary (Odense Fjord, Denmark). Sediments were collected from eight stations within the system and nutrient production and effluxes were measured over a period of $\sim$2 years. Dissolved inorganic nitrogen (DIN) effluxes were high initially but quickly faded to low and stable levels after 50–200 days, whereas PO_4^{3-} effluxes were highly variable in the different sediments. Mineralization patterns suggested that internal N loading would quickly (< 200 days) fade to insignificant levels, whereas internal PO_4^{3-} loading could be sustained for extended time (years). When results from all stations were combined, internal N loading and P loading from the fjord bottom was up to 121×10^3 kg N yr^{-1} (20 kg N ha^{-1} yr^{-1}) and 22×10^3 kg P yr^{-1} (3.6 kg P ha^{-1} yr^{-1}) corresponding to 6 (N) and 36 % (P) of the external nutrient loading to the system. We conclude that the internal N loading resulting from degradation of accumulated ON is low in shallow eutrophic estuaries, whereas microbial mineralization of accumulated OP is a potential source of P. Overall it appears that, in N-limited eutrophic systems, internal nutrient resulting from mineralization of ON and OP in sediments is of minor importance.

1 Introduction

The nutrient loading of coastal ecosystems is often divided into internal and external sources, i.e., release from sediments resulting from organic N (ON) and P (OP) mineralization, and natural and anthropogenic supplies via the water shed and atmospheric deposition, respectively. The external nutrient loading can be quantified by summing up the external sources (e.g., Petersen et al., 2009). It is difficult, however, to use a mass balance approach to obtain reliable estimates of internal nutrient loading, since release from sediments and export to adjacent water bodies are difficult to quantify with sufficient temporal and spatial precision in large and dynamic estuaries with extensive spatial variability and open boundaries.

To complicate matters more, the internal nutrient loading can be divided into two fractions with different temporal dynamics. The first is rapid nutrient release from mineralization of fresh and newly deposited labile organic material, and the second is slow and continued nutrient release from mineralization of buried organic material with lower reactivity. High turnover of labile ON and OP deposited at the sediment–water interface ensures a rapid recycling of inorganic nutrients to the water column (Kelly and Nixon, 1984; Valdemarsen et al., 2009). The primary productivity in many shallow estuaries is therefore partially controlled by nutrients released from the sediments (Cowan and Boynton, 1996; Fullweiler et al., 2010; Mortazavi et al., 2012; Bukaveckas and Isenberg, 2013). The contribution from mineralization of low-reactivity and often deeply buried ON and OP to total sediment nutrient release, however, remains largely unknown. Nutrient release reported in most published studies

is dominated by the nutrients generated by labile ON and OP mineralization due to the short timescale applied for measurements. It is nonetheless important to obtain reliable estimates of the nutrient generation and efflux resulting from mineralization of low-reactivity ON and OP. In many instances the recovery of eutrophic ecosystems after reductions of the external nutrient loading does not occur or only occurs after considerable delay (Kronvang et al., 2005). This may be caused by substantial release of nutrients which have accumulated to high concentrations over time in the sediments exposed to eutrophication (Pitkanen et al., 2001; Carstensen et al., 2006). Such delayed nutrient release is thought to counteract reductions in the external nutrient load and cause delayed recovery.

Determining the magnitude and temporal dynamics of the internal nutrient loading originating from ON and OP accumulated in sediments requires detailed biogeochemical studies. Organic matter degradation in sediments follow exponential decay kinetics (Westrich and Berner, 1984; Burdige, 1991; Valdemarsen et al., 2014), and inorganic nutrient production from ON and OP is therefore expected to decrease exponentially with time. Not all produced inorganic nutrients will result in internal nutrient loading, however, since chemical and biological processes within sediments lead to nutrient retention or transformation before efflux to the overlying water. NH_4^+, for instance, can be adsorbed to the sediment matrix (Mackin and Aller, 1984), assimilated by microbes or benthic microalgae, or microbially transformed to other nitrogenous compounds (Christensen et al., 2000; Tyler et al., 2003; Hulth et al., 2005). Coupled nitrification–denitrification in the oxic–anoxic transition of surface sediments, whereby NH_4^+ is converted to inert N_2 gas, is for instance an ecologically important process which reduces the amount of bioavailable N (Seitzinger, 1988; Burgin and Hamilton, 2007). Due to adsorption and denitrification, the efflux of dissolved inorganic nitrogen ($DIN = NH_4^+ + NO_3^- + NO_2^-$) is generally much lower than anticipated from total ON mineralization in the sediment (Mackin and Swider, 1989). As for NH_4^+, PO_4^{3-} may adsorb to the sediment matrix, mainly to Fe minerals in oxidized surface sediment (Sundby et al., 1992). PO_4^{3-} efflux is therefore generally low in marine sediments lined with an oxic surface layer (Sundby et al., 1992; Jensen et al., 1995; Viktorsson et al., 2013).

In this study an experimental approach was used to determine the internal nutrient loading resulting from long-term mineralization of accumulated ON and OP in various sediment types of a large shallow, eutrophic estuary (Odense Fjord, Denmark). The goals of the study were twofold: (1) to quantify the magnitude and temporal dynamics of internal nutrient loading resulting from mineralization of ON and OP accumulated in sediments and (2) to evaluate the role of internal nutrient loading for the recovery of eutrophic ecosystems. Sediment cores were collected from various locations representing the dominating sediment types and environments in the estuary. These were maintained in experiments lasting ~ 2 years, during which the mineralization of ON and OP and resulting effluxes of inorganic nutrients were measured with high spatial and temporal resolution. By comparing total inorganic nutrient production to effluxes, the fate of inorganic nutrients was elucidated. The total internal nutrient loading of the entire system was estimated based on the measured nutrient effluxes and the areal distribution of dominating sediment types. Finally, the importance of internal nutrient loading in shallow eutrophic ecosystems is evaluated.

2 Materials and methods

2.1 Study area

Odense Fjord is a shallow eutrophic estuary located on the island of Fyn, Denmark. It is divided into a 16 km^2 shallow inner basin and a 45 km^2 deeper outer basin, with average depths of 0.8 and 2.7 m, respectively (Fig. 1). The fjord is connected to Kattegat through a narrow opening in the northeast. The main external nutrient source to Odense Fjord is Odense River, which has a catchment area of 1095 km^2, consisting mainly of farmland and urban areas (Petersen et al., 2009). Odense Fjord was critically eutrophic in the past due to high external nutrient loading exceeding 3000×10^3 kg N yr^{-1} and 300×10^3 kg P yr^{-1} before 1990 (Petersen et al., 2009). The massive nutrient loading caused extensive problems with high pelagic primary production, low water transparency, hypoxic events and blooms of opportunistic macroalgae. Implementation of several water action plans has reduced the external nutrient loading considerably to current levels of about 2000×10^3 kg N yr^{-1} and 60×10^3 kg P yr^{-1}. This has improved the ecological quality of the system, since hypoxia is now rare and levels of opportunistic macroalgae have decreased. Nonetheless, excessive nutrient levels and high primary production are still a problem in Odense Fjord, which may be due to high and sustaining internal nutrient loading.

2.2 Sampling of sediment and water

Intact sediment cores were collected at eight stations from four habitat types in Odense Fjord during October and November 2009 (Fig. 1). The stations were chosen to cover all major sediment types in the fjord: three stations (St 1–3) represented shallow silty sediments in the inner fjord; St 4 and 5 represented shallow (< 1 m) silty and sandy sediments in the outer fjord, respectively; and, finally, three stations (St 6–8) represented deep (2–6 m) silty sediments in the outer fjord. A detailed survey of sediment characteristics conducted in 2009 (partially presented in Valdemarsen et al., 2014) revealed that the four selected habitat types (shallow silty inner fjord, shallow silty outer fjord, shallow sandy outer fjord and deep silty outer fjord) represented 21, 11, 29 and 39 % of the fjord area, respectively. Fifteen sediment

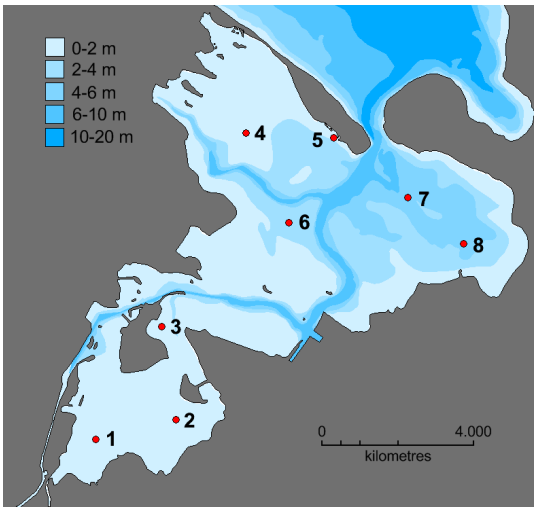

Figure 1. Map of Odense Fjord (55°29′15″ N, 10°31′09″ E) showing the eight stations, where sediments were sampled for the long-term degradation experiment. Gray color indicates land and different shades of blue indicate water depth.

cores were sampled from each station with 30 cm long, 8 cm internal diameter Plexiglas core liners. The shallow stations (St 1–5) were sampled from a dinghy using a hand operated coring device. Cores from the deeper stations (St 6–8) were subsampled from a "HAPS" box corer onboard a larger vessel (*Liv II*, Danish Nature Agency). Water temperatures were 10–12 °C at the time of sampling.

Seawater used for the experiment was collected at Kerteminde Harbor at various times during 2009–2011. The seawater was GF/C-filtered and adjusted to the appropriate salinity (10 or 20) before it was used for experiments.

2.3 Experimental setup

Sediment cores were pre-treated before the experiment to assure that they had equal sediment height and were free of macrofauna. The sediment cores were adjusted to 20 cm depth by removing the bottom stopper and carefully removing excess sediment from below. After reinserting the bottom stopper, the overlying water was purged with N_2 for 30 min to induce anoxia and the top stopper was reinserted. Asphyxiated macrofauna was removed from the sediment surface after ∼ 48 h in darkness.

The pre-treatment was completed 2–4 days after sampling and sediment cores were then transferred to the experimental setup consisting of eight ∼ 70 L water tanks located in a temperature-controlled room at 15 °C. The incubation temperature of 15 °C approximately corresponds to the average annual water temperature in Odense Fjord. Each tank contained all sediment cores from one station and was filled with filtered seawater with a salinity of 10 for St 1–3 and salinity of 20 for St 4–8, corresponding to the average salinity in the inner and outer basins of Odense Fjord (Fyns Amt, 2006). The water reservoir in each tank was vigorously mixed and aerated by air pumps, and kept at a level 0.5 cm above the upper rim of the open core liners to assure mixing of the headspace. The tanks were kept in darkness and about one-third of the water was renewed with fresh seawater every 2 weeks.

The sediment cores were maintained in this setup for the entire experiment, which lasted 589–635 days, depending at station. The time when cores were first transferred to the incubation tanks is referred to as $t = 0$. At selected times, three random sediment cores from each station were temporarily removed for flux measurements, and at other times three sediment cores were removed permanently for porewater and solid-phase analysis as well as anoxic sediment incubations (for more detail see sections below).

2.4 Flux measurements

The net exchange of nutrients (DIN and PO_4^{3-}) between sediment and water was determined in flux experiments with three random sediment cores from each station. Flux experiments were conducted weekly during the first 30 days, monthly until day 180 and every 2–3 months to the end. One day prior to flux measurements, the inside headspace wall of the cores designated for flux measurements were cleaned with a cotton swab to avoid biased flux measurements resulting from bacterial biofilms on the inner surface of core liners (Valdemarsen and Kristensen, 2005). These cores were removed from the incubation tanks the next day, equipped with 4 cm long magnetic stirring bars a few centimeters above the sediment surface and placed around a central magnet rotating at 60 rpm. Initial water samples were taken from all cores before they were closed with rubber stoppers. The cores were incubated in darkness for 4 h initially and up to 24 h at the end of the experiment, before the rubber stoppers were removed and final water samples were taken. Nutrient samples were stored frozen (−20 °C) until analyzed for NH_4^+, NO_x^- ($NO_3^- + NO_2^-$) and PO_4^{3-} on a Lachat Quickchem 8500 flow injection analyzer.

2.5 Core sectioning

Three sediment cores from each station were sectioned into 2 cm intervals to 16 cm depth at various times (after 1 day and 1, 7–8, 16–17 and 20–21 months). Core sectioning and subsequent sediment and porewater handling was done inside a N_2-filled glovebag. Individual sediment slices were homogenized and porewater for nutrient analysis was obtained after centrifugation of sediment subsamples in double centrifuge tubes (10 min, ∼ 500 g) and GF/C filtration. Samples for NH_4^+ and PO_4^{3-} were stored frozen (−20 °C) until analysis as described above.

Sediment characteristics were determined on subsamples from every depth interval during the core sectioning on day 1. Grain size composition, loss on ignition (LOI), total organic

C (TOC) content, density and porosity were determined as described in Valdemarsen et al. (2014). Total N (TN) was measured by elemental analysis on dried sediment subsamples on a Carlo Erba CHN EA1108 elemental analyzer. Total P (TP) was extracted by boiling combusted sediment subsamples for 1 h in 1 M HCl. After centrifugation (10 min, 500 g) the supernatants were stored until analyzed for PO_4^{3-} by colorimetric analysis (Koroleff, 1983).

During initial and final core sectionings, reactive Fe was extracted from ∼ 0.2 g sediment subsamples with 0.5 M HCl. After 30 min extraction on a shaking table and centrifugation (10 min, 500 g) the supernatants were stored in 4 mL plastic vials at room temperature until analysis. Supernatants were analyzed for reduced Fe (FeII) and total Fe using the ferrozine method before and after reduction with hydroxylamine (Stookey, 1970; Lovley and Phillips, 1987). Oxidized iron (FeIII) was determined as the difference between total Fe and FeII.

Linear dimensionless NH_4^+-adsorption coefficients were determined during the initial core sectioning on wet sediment subsamples from 0–2, 4–6 and 8–10 cm depth intervals in NH_4^+-adsorption experiments as described in Holmboe and Kristensen (2002). Sediment subsamples were incubated for 2 days in slurries with different NH_4^+ concentrations (0, 1, 2 and 3 mM) and 10 mg L^{-1} allylthiourea to inhibit nitrification. After centrifugation (10 min, 500 g) the supernatant was decanted and adsorbed NH_4^+ was extracted from the sediment pellet in 2 M KCl (Mackin and Aller, 1984). Supernatants from slurries and KCl extractions was stored frozen (−20 °C) and analyzed for NH_4^+ using the salicylate–hypochlorite method (Bower and Holm-Hansen, 1980).

2.6 Jar experiments

Closed anoxic sediment incubations ("jar experiments") were performed with sediment from different depths (0–2, 4–6 and 8–10 cm) right after core sectionings. Jar experiments measure the total anaerobic mineralization rates of ON and OP from temporal accumulation of metabolic end products (NH_4^+ and PO_4^{3-}) in the porewater and yields solid results under a wide range of environmental and experimental conditions (Kristensen and Hansen, 1995; Kristensen et al., 2011; Valdemarsen et al., 2012; Quintana et al., 2013). Sediment from different depths was homogenized and fully packed into 6–8 glass scintillation vials ("jars"), leaving no headspace. The jars were closed with screw caps and buried in anoxic sediment at 15 °C. Two jars were sacrificed at 3–5 day intervals for porewater extraction by centrifugation. The jars were fitted with a perforated lid containing a GF/C filter inside before centrifugation and were then centrifuged head-down in a centrifuge tube (10 min, ∼ 500 g). Extracted porewater was stored frozen (−20 °C) and analyzed for NH_4^+ and PO_4^{3-} by colorimetric analysis as described above.

2.7 Calculations and statistics

Initial area-specific pools of TN and TP were calculated by depth integration (0–20 cm) of TN and TP content in individual sediment layers. Differences in area-specific pools of TN and TP between stations were detected by one-way ANOVA followed by Tuckey's post hoc test. Data were log-transformed before statistical analysis when assumptions of homoscedasticity were not met (only TN). Area-specific pools of FeIII were calculated by depth integration at the beginning (initial) and end (final) and compared by pairwise *t* tests.

NH_4^+-adsorption coefficients (K_{NH}) in individual sediment layers were determined based on NH_4^+-adsorption experiments. Extracted NH_4^+ (µmol g dw sediment) was plotted against NH_4^+ concentration (µmol cm^{-3}), and the linear slope, K', was determined by least-squares regression. K_{NH} could hereafter be determined from the relationship $K_{NH} = ((1-\Phi)/\Phi) \times \rho_{ds} \times K'$, where Φ is sediment porosity and ρ_{ds} is dry sediment density (Holmboe and Kristensen, 2002).

Rates of microbial ON and OP mineralization in discrete depth intervals (0–2, 4–6 and 8–10 cm) were obtained from jar experiments by fitting the time-dependent linear concentration change of NH_4^+ and PO_4^{3-} by least-squares regression (Aller and Yingst, 1980). When slopes were significant ($p < 0.05$) the volume-specific reaction rates (nmol cm^{-3} d^{-1}) in individual depth layers were calculated from the slopes and corrected for sediment porosity and adsorption (Kristensen and Hansen, 1995). The mineralization rates at 10–20 cm depth were calculated from exponential regressions based on ON and OP mineralization rates in the top 10 cm. Total area-specific ON and OP mineralization was calculated by depth integration (0–20 cm) of measured NH_4^+ and PO_4^{3-} production at different depths. The temporal patterns of total area-specific ON and OP mineralization were fitted to a double exponential decay regression model of the form $y = C_L \times \exp(-k_L \times t) + C_R \times \exp(-k_R \times t)$, where t is time, C_L and C_R are constants and k_L and k_R denote the first-order decay constants for labile and refractory ON and OP, respectively. We hereby assume that considerations based on organic C degradation kinetics (Westrich and Berner, 1984) are also valid for ON and OP mineralization. Half-lives of labile and refractory ON and OP could hereafter be calculated from the formula $T_{0.5} = \ln(2)/k'$, where k' denote k_L and k_R.

3 Results

3.1 Sediment characteristics

Detailed sediment characteristics of the eight stations in Odense Fjord were previously described in Valdemarsen et al. (2014) and only a brief summary is given here. The sed-

Table 1. Dimensionless linear NH_4^+-adsorption coefficients, K_{NH}, for different sediment depths at St 1–8.

	St 1	St 2	St 3	St 4	St 5	St 6	St 7	St 8
0–2 cm	0.26	1.06	0.33	0.46	0.64	0.31	0.57	0.48
6–8 cm	0.52	0.76	0.49	0.45	0.82	0.51	0.62	0.36
8–10 cm	0.40	0.82	0.20	0.79	0.55	0.66	0.14	0.45

Table 2. Depth-integrated (0–16 cm) area-specific TN and TP content ± SE ($n = 3$) at St 1–8. Superscript letters indicate the grouping of data obtained by ANOVA and subsequent post hoc analysis. Average TN : TP ratios are also shown.

	TN	TP	TN : TP
	(mol m^{-2})	(mol m^{-2})	–
St 1	13.5 ± 0.4^a	1.34 ± 0.04^a	10.1
St 2	21.5 ± 0.5^b	1.31 ± 0.02^a	16.4
St 3	16.0 ± 0.2^b	0.70 ± 0.06^b	22.9
St 4	16.6 ± 1.1^b	1.18 ± 0.06^a	14.1
St 5	4.5 ± 0.1^c	0.73 ± 0.04^b	6.2
St 6	17.1 ± 0.1^b	1.94 ± 0.03^c	8.8
St 7	18.1 ± 0.0^b	1.86 ± 0.05^c	9.7
St 8	19.5 ± 0.2^b	1.83 ± 0.03^c	10.7

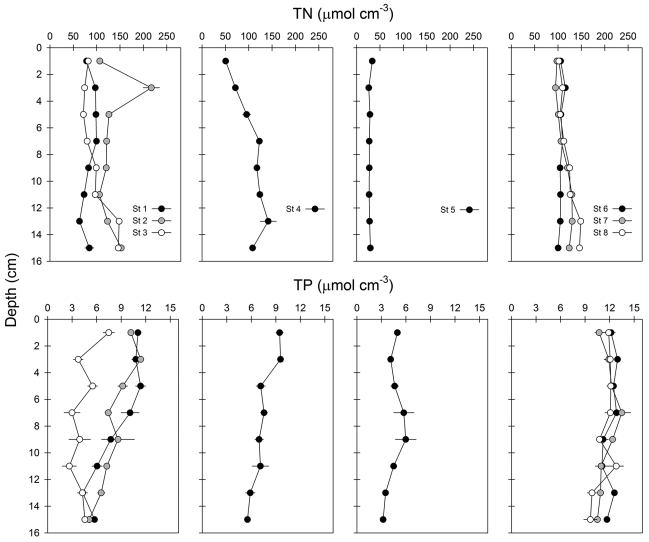

Figure 2. Total nitrogen (TN) and total phosphorous (TP) in sediments from Odense Fjord. Left panels show stations from the shallow inner fjord (St 1, 2 and 3), middle panels show shallow silty and sandy sediments in the outer fjord (St 4 and 5, respectively) and right panels show deep silty sediments in the outer fjord (St 6, 7 and 8). Error bars indicate standard error ($n = 3$).

iments from all stations had high sand content and variable silt–clay content with wet densities ranging from 1.2 to 1.8 g cm^{-3} and porosities of 0.3–0.8. The medium grain size varied from 87 to 397 µm among stations. The sediments from the innermost stations (St 1–3) and most of the stations in the outer basin (St 4 and 6–8) contained a high proportion of silt–clay particles (13–63 %). Furthermore, the stations rich in silt–clay particles were organic rich with 0.6–5.2 % POC compared to the more sandy St 5 (0.1–0.2 % POC).

NH_4^+-adsorption coefficients varied erratically among stations and sediment depths (Table 1). K_{NH} ranged from 0.14 in the 8–10 cm deep sediment at St 7 to 1.06 in the surface sediment at St 2.

St 1 and St 3 from the inner basin had similar TN content ranging between 57 and 156 µmol cm^{-3} (Fig. 2). St 2 had slightly higher TN (103–227 µmol cm^{-3}) with a pronounced subsurface peak occurring at 3 cm depth. In the outer basin the shallow and deep silty stations (St 4 and 6–8) had similar TN content (92–154 µmol cm^{-3}), except at the surface, where TN was lower at St 4 (38–60 µmol cm^{-3}). The sandy St 5 contained exceptionally low TN (8–16 µmol cm^{-3}). Depth-integrated TN was therefore lowest at St 5 (4.5 ± 0.1 mol N m^{-2}), intermediate at St 1 (13.5 ± 0.4 mol N m^{-2}) and similarly high at the remaining stations (16.0 to 21.4 mol N m^{-2}, Table 2).

Two of the stations in the inner basin (St 1 and 2) had similar TP profiles, with 10–11 µmol cm^{-3} at the sediment surface and a gradual decrease to 5.1–5.8 µmol cm^{-3} at 15 cm depth (Fig. 2). St 3 had the lowest TP content of the stations in the inner basin. The shallow silty sediments in the outer basin (St 4) were similar to St 1–2 with respect to TP, whereas the shallow sandy sediment (St 5) was similar to St 3. The deep silty sediments in the outer basin (St 6–8) were characterized by constant TP with depth (9.6–13.5 µmol cm^{-3}). Depth integration showed that the highest area-specific TP content was found at the deep outer fjord stations (1.8–1.9 mol P m^{-2}), whereas shallow silty sediments in the inner and outer fjord contained intermediate TP content (1.2–1.3 mol P m^{-2}; St 1, 2 and 4; Table 2). The lowest TP content (~ 0.7 mol P m^{-2}) was found at the silty St 3 and sandy St 5 in inner and outer fjord, respectively.

Initial FeIII pools varied 30-fold between stations (6–243 mmol m^{-2}; Table 3), with the lowest FeIII content found in shallow sandy sediment from the outer basin (St 5). FeIII only constituted a minor fraction (2–10 %) of total Fe at all stations. No statistically significant differences were detected between initial and final FeIII pools ($p > 0.17$), but there were trends towards higher final FeIII content, except at St 1 and 5.

3.2 ON and OP mineralization

Mineralization rates obtained in the fully anoxic jar experiments might have underestimated mineralization rates at the sediment surface, where O_2 can stimulate mineralization of O_2-sensitive organic matter (Hulthe et al., 1998). In coastal and estuarine sediments, O_2 only penetrates to 1–3 mm depth, suggesting a minor importance of this artifact at the beginning of the experiment. Surprisingly, the sedi-

Table 3. Initial and final depth-integrated pools (0–20 cm) of FeIII ± SE ($n = 3$) at St 1–8. t tests showed no significant difference between initial and final FeIII pools at any station.

	Initial		Final	
	FeII (mmol m^{-2})	FeIII (mmol m^{-2})	FeII (mmol m^{-2})	FeIII (mmol m^{-2})
St 1	2390 ± 34	243 ± 24	2294 ± 153	92 ± 22
St 2	2302 ± 160	157 ± 32	2399 ± 189	271 ± 161
St 3	1356 ± 155	62 ± 25	1358 ± 154	109 ± 40
St 4	1054 ± 86	28 ± 20	996 ± 23	97 ± 37
St 5	258 ± 2	6.3 ± 1.0	274 ± 39	6.4 ± 1.2
St 6	1887 ± 37	75 ± 12	1813 ± 43	141 ± 40
St 7	2464 ± 105	52 ± 2.0	2142 ± 60	137 ± 48
St 8	1697 ± 63	156 ± 8.0	1813 ± 43	210 ± 89

ments did not become significantly more oxidized during the long-term incubations as indicated by a modest buildup of oxidized FeIII and continuous presence of hydrogen sulfide in the porewater of surface sediment from all stations (data not shown). Hence we assume that mineralization rates in the sediment cores underlying an oxic water phase were closely approximated by the rates obtained in jar experiments.

NH_4^+ production in jar experiments was significant throughout the experiment, except for St 1, 8–10 cm depth after 607 days. Initially NH_4^+ production was highest in the surface 0–2 cm sediment from the silty St 1–2 in the inner fjord and the sandy St 5 in the outer fjord (159–338 nmol cm^{-3} d^{-1}) and was similar at remaining stations (63–101 nmol cm^{-3} d^{-1}; Fig. 3). Surface NH_4^+ production decreased rapidly over time in sediments from shallow locations in the inner and outer fjord, by 96 % of initial rates at St 1 and by 61–82 % at St 2–5. The surface NH_4^+ production in the sediments sampled in the deep outer basin (St 6–8) decreased by 8–67 % during the experiment. NH_4^+ production at 4–6 cm depth was initially 18–60 nmol cm^{-3} d^{-1} at all stations and temporal changes were also observed in this layer, especially in shallow silty sediments from the inner basin, where NH_4^+ production decreased by 75–96 % to 1.4–12 nmol cm^{-3} d^{-1} by the end (Fig. 3). In sediments from the outer basin, NH_4^+ production at 4–6 cm depth only decreased by 19–58 %. At 8–10 cm depth, NH_4^+ production at all stations occurred at similar rates and showed similar temporal trends as observed at 4–6 cm depth (Fig. 3).

Significant PO_4^{3-} production was measured in the surface sediment from all stations throughout the experiment (Fig. 4). Initial rates were highest (30–35 nmol cm^{-3} d^{-1}) at St 1 and 2 from the shallow inner basin and considerably lower (7–18 nmol cm^{-3} d^{-1}) at the remaining stations. PO_4^{3-} production initially decreased rapidly in the surface sediment from St 1 and 2 and stabilized at relatively low and stable levels after ∼ 200 days (0.7–6.0 nmol cm^{-3} d^{-1}). Surface PO_4^{3-} production also decreased over time at the other stations, but temporal trends were more erratic. PO_4^{3-} production in deeper sediment was generally lower than at the surface, and with less variability among stations (Fig. 4). PO_4^{3-} production at 4–6 cm depth was 0–6 nmol cm^{-3} d^{-1} and remained quite stable throughout the experiment at all stations. The only significant decrease ($p = 0.01$–0.03) occurred in silty sediments from the inner basin (St 1–3) and St 6 and 8 from the deep outer basin. PO_4^{3-} production varied between 0 and 5 nmol cm^{-3} d^{-1} at 8–10 cm depth and was stable throughout the experiment.

Area-specific ON mineralization was calculated by depth integration of NH_4^+ production rates (Fig. 3). The sediments from the inner basin (St 1–3) showed high initial ON mineralization (6–11 mmol m^{-2} d^{-1}) in the same range as the shallow silty and sandy sediments from the outer basin (6 and 10 mmol m^{-2} d^{-1} at St 4 and 5, respectively). The deep silty sediments from the outer basin showed the lowest initial ON mineralization (St 6–8; 3–5 mmol m^{-2} d^{-1}). Area-specific ON mineralization decreased during the experiment at all stations, by 82–93 % for the silty inner fjord and 34–71 % at remaining stations. The temporal decrease was mainly driven by successively lower ON mineralization in surface sediment during the first ∼ 200 days and area-specific ON mineralization was fairly constant hereafter. Initial area-specific OP mineralization was 0.2–1.0 mmol m^{-2} d^{-1} (Fig. 4) and decreased (59–70 %) over time at several of the stations (St 1–3 and St 6). As for ON mineralization, the successively lower OP mineralization was mainly due to decreased OP mineralization in surface sediment. At the other stations area-specific OP mineralization remained relatively high and did not show clear temporal trends.

Double exponential decay models fitted the ON mineralization kinetics at St 1–6 and the OP mineralization kinetics at St 1–3 and 6. Erratic mineralization patterns prevented the use of exponential decay models at remaining stations (see Fig. 3–4). Decay constants for labile and refractory ON and OP in were fairly similar at all stations, with k_L's of 0.02–0.06 d^{-1} (except for 10 times higher values for ON at St 6 and for OP at St 2) and k_R's of 0.0003–0.0015 (Table 4). The half-lives for ON and OP were in the range of 0.01–0.11 and 1.3–6.3 years for labile and refractory fractions, respectively.

3.3 DIN and DIP fluxes

DIN fluxes followed a similar exponentially decreasing pattern for all stations (Fig. 5), and ranged from 1.1–3.7 mmol m^{-2} d^{-1} initially ($t = 0$–90 d) to 0.09–0.5 mmol m^{-2} d^{-1} by the end. The main form of DIN released initially was NH_4^+, which contributed 59–100 % of DIN release. Subsequently the NH_4^+ efflux decreased, while NO_x^- switched from uptake to release, and after 0.5–1 years to the end of the experiment, 68–100 % of the DIN was released as NO_x^-.

The eight stations showed different patterns of PO_4^{3-} fluxes. The stations from the shallow inner basin, St 1–3, showed exponentially decreasing PO_4^{3-} fluxes over time

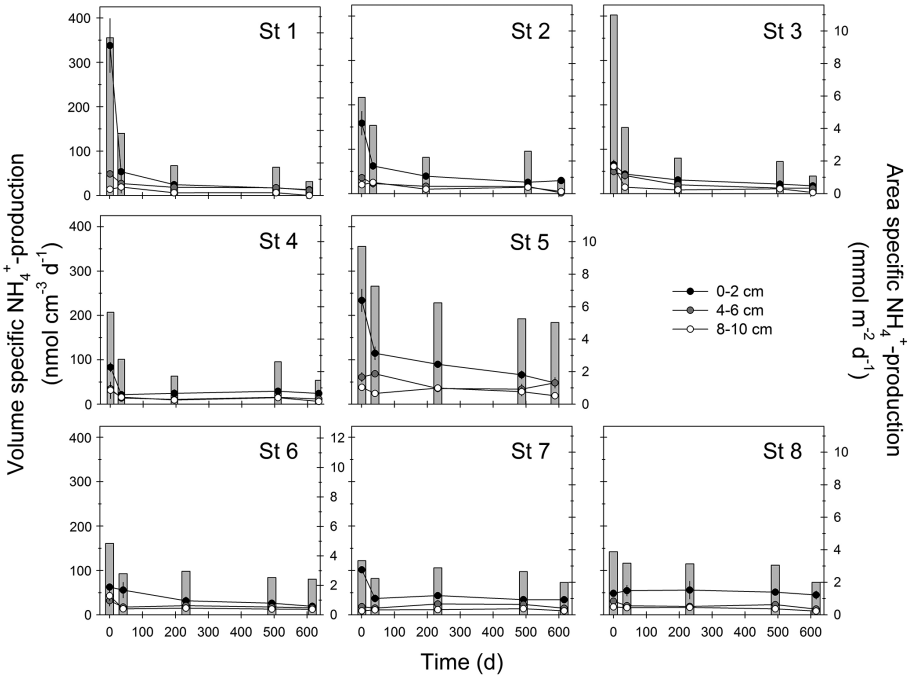

Figure 3. NH_4^+ production measured in jar experiments with sediment from shallow inner basin (upper panels), shallow silty and sandy outer basin (middle panels) and deep silty outer basin (lower panels). Black, gray and white symbols indicate volume-specific NH_4^+ production in sediment from 0–2, 4–6 and 8–10 cm depth, respectively (left *y* axis). Bars indicate depth-integrated (0–20 cm) NH_4^+ production based on volume-specific production rates (right *y* axis).

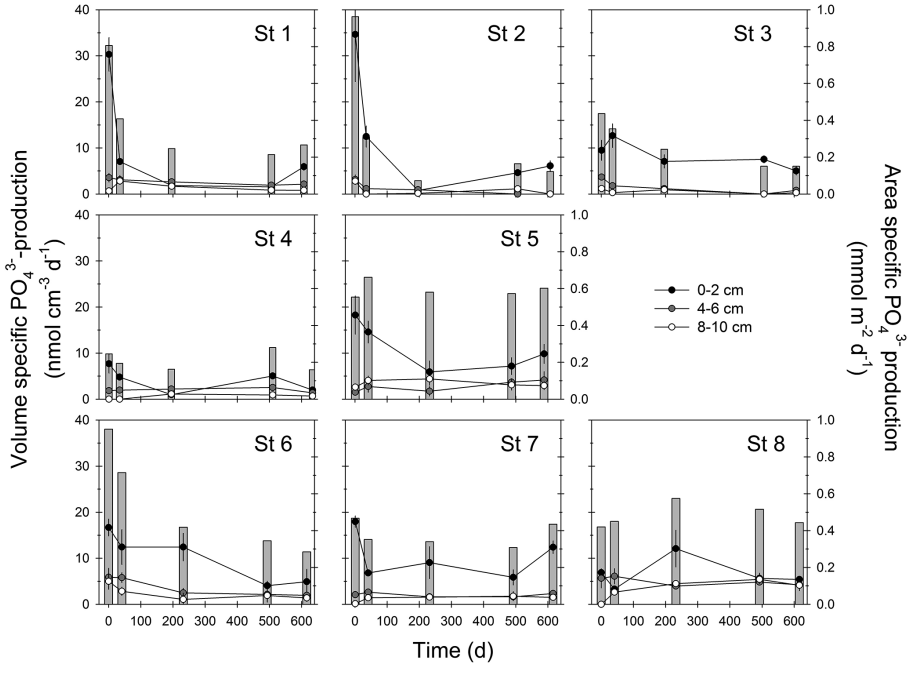

Figure 4. PO_4^{3-} production measured in jar experiments performed with sediment from shallow inner fjord (upper panels), shallow silty and sandy outer fjord (middle panels) and deep silty outer fjord (lower panels). Black, gray and white symbols indicate volume-specific PO_4^{3-} production in sediment from 0–2, 4–6 and 8–10 cm depth, respectively (left *y* axis). Bars indicate depth-integrated (0–20 cm) PO_3^{3-} production based on volume-specific production rates (right *y* axis).

Table 4. Double exponential regression statistics for the temporal trends of total ON and OP degradation in jar experiments. Total organic N (ON) and P (OP) degradation were fitted to the exponential decay function $y = C_L \times \exp(-k_L \times x) + C_R \times \exp(-k_R \times x)$, where C_L and C_R denote constants and k_L and k_R denote decay constants for labile and refractory organic ON and OP, respectively. Statistics were not calculated for St 7–8 (ON) and for St 4–5 and 7–8 (OP), since the temporal degradation patterns did not fit the double exponential decay model. $T_{L,\,0.5}$, and $T_{R,\,0.5}$, denote the half-life (y) of labile and refractory ON and OP, respectively.

ON						
	k_L	k_R	C_L	C_R	$T_{L,\,0.5}$	$T_{R,\,0.5}$
St 1	4.6×10^{-2}	1.1×10^{-3}	7.7	2.4	0.04	1.73
St 2	2.3×10^{-2}	1.0×10^{-3}	3.1	2.9	0.08	1.90
St 3	5.3×10^{-2}	1.1×10^{-3}	8.6	2.8	0.04	1.73
St 4	4.3×10^{-2}	0.4×10^{-3}	4.0	1.8	0.04	4.75
St 5	5.7×10^{-2}	0.6×10^{-3}	2.7	7.2	0.03	3.17
St 6	52.4×10^{-2}	0.3×10^{-3}	3.2	2.9	0.01	6.33
St 7	–	–	–	–	–	–
St 8	–	–	–	–	–	–

OP						
	k_L	k_R	C_L	C_R	$T_{L,\,0.5}$	$T_{R,\,0.5}$
St 1	3.9×10^{-2}	0.4×10^{-3}	0.6	0.3	0.05	4.75
St 2	56.0×10^{-2}	1.5×10^{-3}	1.1	0.3	0.01	1.27
St 3	2.2×10^{-2}	1.3×10^{-3}	0.1	0.3	0.08	1.46
St 4	–	–	–	–	–	–
St 5	–	–	–	–	–	–
St 6	1.7×10^{-2}	0.9×10^{-3}	0.4	0.5	0.11	2.11
St 7	–	–	–	–	–	–
St 8	–	–	–	–	–	–

(initial fluxes of 0.1–0.2 mmol m^{-2} d^{-1} decreasing to 0.01–0.05 mmol m^{-2} d^{-1} by the end; Fig. 5). Initial (day 0–90) PO_4^{3-} fluxes at the shallow silty St 4 was around zero, but increased to 0.07–0.14 mmol m^{-2} d^{-1} during days 90–360 of the experiment. The highest PO_4^{3-} fluxes (0.07–0.21 mmol m^{-2} d^{-1}) were observed at the TP-poor sandy St 5, particularly towards the end of the experiment, while the TP-rich outer fjord stations 6–8 had the lowest and most irregular PO_4^{3-} fluxes, ranging from slightly negative to 0.1 mmol m^{-2} d^{-1}.

3.4 PO_4^{3-} and NH_4^+ in porewater

Porewater nutrient concentrations increased gradually at all depths during the experiment (data not shown). NH_4^+ and PO_4^{3-} only increased moderately in the upper 2 cm, but accumulated to high levels in the deeper diffusion-limited sediment. Depth-averaged initial porewater NH_4^+ concentration varied between 171 and 407 µM at the stations. The sandy St 5 showed the highest NH_4^+ accumulation over time with a depth average of 1473 µM in porewater by the end. At the remaining stations, NH_4^+ only accumulated to 259–587 µM. Depth-averaged PO_4^{3-} concentrations at the beginning varied between 17 and 71 µM depending on station. As for NH_4^+, the nutrient-poor sandy St 5 showed the highest PO_4^{3-} accumulation to 368 µM compared with 43–170 µM at the other stations.

3.5 N and P budgets

Area-specific nutrient mineralization obtained in jar experiments was used to calculate total ON and OP mineralization during the experiment. ON mineralization was fairly constant for all stations except St 5 (1.4 to 1.9 mol m^{-2}), corresponding to 8–10 % of initial TN (Table 5). St 5, on the other hand, had 3-fold higher ON mineralization that accounted for 80 % of the initial ON. A 3-fold range among stations was also evident for OP mineralization, but with lowest rates of 0.12–0.l8 mol m^{-2} at St 1–4 and the highest rates of 0.22–0.33 mol m^{-2} at St 5–8 (8–48 % of initial TP). Interestingly, there was no apparent relationship between sediment TN and TP content and mineralization activity, as some of the highest N and P mineralization rates were observed at the organic-poor St 5 (Table 4). DIN effluxes, porewater accumulation and adsorption only accounted for 18–32 % of total ON mineralization, indicating that most of the generated NH_4^+ was not accounted for by our measurements. For P, the sum of

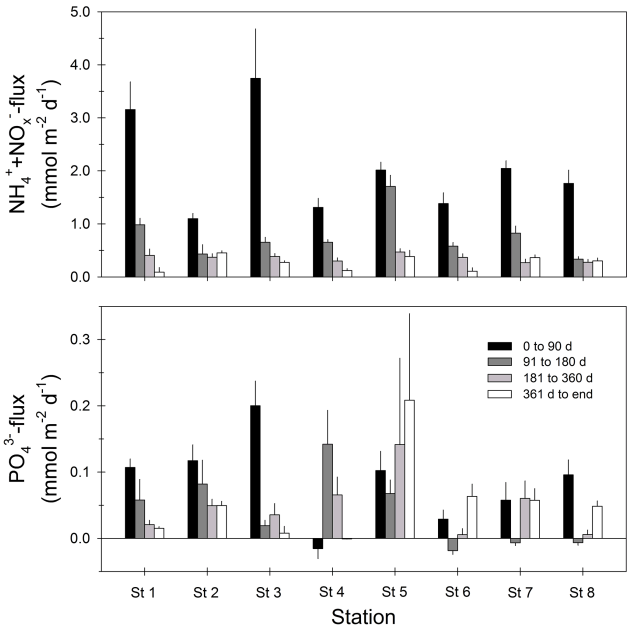

Figure 5. Fluxes of dissolved inorganic nitrogen ($DIN = NH_4^+ + NO_x^-$) and PO_4^{3-} at various times during the experiment. Error bars represent standard error ($n = 6$–24).

PO_4^{3-} efflux and porewater accumulation only accounted for 10–48 % of total OP mineralization.

4 Discussion

4.1 Sediment nutrient content

TN and TP in sediments from Odense Fjord were in the same range or higher than reported for other eutrophic systems (e.g., Boynton and Kemp, 1985; Cowan and Boynton, 1996; Lomstein et al., 1998; Coelho et al., 2002; Viktorsson et al., 2013), emphasizing the history of intense eutrophication in Odense Fjord. TN and TP in the silty sediments of Odense Fjord (all stations except St 5) were remarkably similar and only varied ∼ 1.5-fold (TN) and ∼ 3-fold (TP) among stations. Despite these overall similarities, the silty sediments from the shallow inner basin showed higher initial ON and OP mineralization and nutrient effluxes than silty sediments from the outer fjord. This could be due to higher availability of labile ON and OP in the sediments from the inner basin, reflecting the nutrient-rich conditions in the inner compared to the outer basin (Petersen et al., 2009).

The sandy St 5 was markedly different from the other stations. It had the lowest total nutrient content and yet exhibited some of the highest rates of ON and OP mineralization. The frequent erosion by wind-driven waves in this area (Valdemarsen et al., 2010) and deep (> 20 cm) reworking by lugworms (*Arenicola marina*; Riisgaard and Banta, 1998; Valdemarsen et al., 2011) may remove fine particles and refractory organic matter from St 5 sediments (Wendelboe et al., 2013) and prevent organic matter accumulation, hence explaining the low organic content at this station. On the other hand, intense growth and burial of microphytobenthos and other reactive detritus by the strong physical disturbance and vertical mixing can explain the unexpectedly high TN and TP reactivity of St 5 sediment.

A rough areal estimate based on the measured TN and TP content at the examined stations (Table 2) suggests that 12.6×10^6 kg N and 3.7×10^6 kg P are stored in the upper 20 cm of Odense Fjord sediments, corresponding to ∼ 6 (N) and ∼ 62 (P) years of the current annual external nutrient loading to the system.

4.2 Organic N and P mineralization

Microbial mineralization of ON and OP in Odense Fjord sediments led to marked release of inorganic nutrients, especially in the initial phase of the experiment. Initially there were strong vertical gradients of ON and OP mineralization in silty and sandy sediments from shallow environments, indicating that newly deposited and relatively labile organic matter was being degraded near the sediment surface, with the depth gradient reflecting a gradual and time-dependent depletion of labile ON and OP (Westrich and Berner, 1984; Mackin and Swider, 1989; Valdemarsen et al., 2014). It was expected that ON and OP mineralization would decrease with time at all depths due to diminishing reactivity of the organic pools. However, significant temporal decreases were only observed in surface sediments from shallow locations, whereas mineralization rates were surprisingly stable in the underlying sediment and the entire sediment column in the deep outer fjord. Assuming that organic matter degradation follows an exponential decay pattern, the lack of a detectable attenuation in mineralization rates over a ∼ 2-year period indicates very low initial reactivity of ON and OP in the deeper layers (Westrich and Berner, 1984). Nevertheless, since ON and OP of low reactivity was present at high concentrations, it remained a significant source for inorganic nutrients.

Total jar-based microbial ON and OP mineralization over the ∼ 2-year experimental period (Table 5) only accounted for a minor fraction of initial TN and TP in sediments from Odense Fjord, suggesting that the standing stock of organic N and P will be a source of nutrients for extended time. Decay constants from the exponential decay model suggested that labile ON and OP was rapidly degraded at all stations within 10–240 days, whereas depletion of more refractory ON and OP will only occur on decadal timescales (8–40 years), indicating that depletion of buried and degradable ON and OP in eutrophic ecosystems will take considerable time.

Table 5. N and P budgets for the experiment. Initial TN and TP are the depth-integrated values based on initial measurements. ON and OP degradation were calculated based on area-specific rates obtained from jar experiments. Total NH_4^+, NO_x^- and PO_4^{3-} effluxes were calculated by time integration of effluxes over the entire experimental period. NH_4^+ and PO_4^{3-} accumulation in porewater (pw) was calculated from the difference between initial and final pw profiles. NH_4^+ adsorption was calculated from initial and final pw inventories of NH_4^+ and the average NH_4^+-adsorption coefficient for each station. Values in parentheses marked with * or ** represent percentage relative to initial TN and TP or total N and P mineralization, respectively.

N mineralization	St 1	St 2	St 3	St 4	St 5	St 6	St 7	St 8
Initial TN (mol m^{-2})	13.5	21.5	16.0	16.6	4.5	17.1	18.1	19.5
ON degradation, jars (mol m^{-2})*	1.38	1.62	1.56	1.44	3.62	1.77	1.61	1.86
	(10.2)	(7.5)	(9.8)	(8.6)	(80.1)	(10.1)	(8.9)	(9.6)
NH_4^+ efflux (mol m^{-2})**	0.26	0.10	0.23	0.15	0.38	0.09	0.27	0.12
	(19.1)	(6.2)	(14.6)	(10.7)	(10.6)	(5.1)	(16.6)	(6.2)
NO_x^- efflux (mol m^{-2})**	0.15	0.21	0.19	0.11	0.18	0.22	0.17	0.20
	(11.2)	(13.0)	(12.1)	(7.3)	(5.0)	(12.9)	(10.8)	(10.9)
NH_4^+ accumulation, pw (mol m^{-2})**	0.02	0.01	0.00	0.08	0.06	0.03	0.01	0.02
	(1.6)	(0.7)	(0.0)	(5.9)	(1.6)	(1.8)	(0.7)	(1.3)
NH_4^+ adsorption (mol m^{-2})**	0.01	0.01	0.00	0.01	0.04	0.02	0.00	0.01
	(0.7)	(0.6)	(0.0)	(0.4)	(1.0)	(1.0)	(0.2)	(0.6)
P mineralization	St 1	St 2	St 3	St 4	St 5	St 6	St 7	St 8
Initial TP (mol m^{-2})	1.34	1.31	0.70	1.18	0.73	1.94	1.86	1.83
OP degradation, jars (mol m^{-2})*	0.16	0.12	0.18	0.13	0.29	0.28	0.22	0.33
	(12.6)	(7.9)	(19.6)	(11.2)	(47.7)	(14.5)	(11.5)	(17.4)
PO_4^{3-} efflux (mol m^{-2})**	0.02	0.04	0.02	0.02	0.10	0.02	0.03	0.02
	(12.6)	(38.0)	(16.8)	(15.8)	(27.8)	(7.4)	(12.8)	(6.5)
PO_4^{3-} accumulation, pw (mol m^{-2})**	0.01	0.01	0.00	0.00	0.02	0.01	0.00	0.01
	(4.8)	(9.6)	(1.6)	(0.8)	(5.1)	(3.0)	(1.7)	(3.1)

4.3 Fate of inorganic nutrients

NH_4^+ and PO_4^{3-} produced by microbial mineralization accumulated in porewater of all sediments within the first 1–6 months and only changed slightly hereafter. However, over the whole experiment, porewater accumulation explained only a minor fraction of the jar-based total ON and OP mineralization (0.8–8.1 %). We also investigated whether NH_4^+ adsorption to mineral surfaces was an important N sink. Despite the large spatial heterogeneity of NH_4^+ adsorption, this process never accounted for more than 1 % of the total produced NH_4^+ over the whole experiment and was therefore not quantitatively important.

Nutrient release to the overlying water was the most important route for inorganic nutrients produced by microbial mineralization. We could not account for all the produced nutrients, since nutrient mineralization in jar experiments exceeded DIN and PO_4^{3-} effluxes by 70–84 % and 62–93 %, respectively. The missing NH_4^+ may have been lost through coupled nitrification–denitrification (e.g., Mackin and Swider, 1989; Quintana et al., 2013). The conspicuous shift from NH_4^+ to NO_3^- release indicated that nitrification was an active process in all sediment types, and denitrifying bacteria probably proliferated in the NO_3^--rich surface sediment. In the present case, coupled nitrification–denitrification rates of 1–2 mmol m^{-2} d^{-1} are required to account for the missing NH_4^+, which is within the range reported in previous studies (e.g., Nielsen and Rasmussen, 1995; Christensen et al., 2000; Tobias et al., 2003). On the other hand, the missing PO_4^{3-} must have been retained within the sediments. Several studies suggest almost complete PO_4^{3-} retention in marine sediments with an oxic sediment surface (Rozan et al., 2002; Viktorsson et al., 2013) where PO_4^{3-} adsorbs to oxidized FeIII minerals, preventing PO_4^{3-} efflux (Sundby et al., 1992). Experimental studies suggest that every FeIII molecule can retain more than 0.5 PO_4^{3-} molecules (Gunners and Blomqvist, 1997; Rozan et al., 2002). Hence the FeIII levels at all the silty stations were sufficient to retain the missing PO_4^{3-}, especially when considering that 0.5 M HCl extractions only extracts a fraction of the available FeIII. At the sandy St 5 the FeIII levels were too low to account for the missing PO_4^{3-}, indicating that there were other PO_4^{3-} sinks. PO_4^{3-} adsorption in the anoxic sediment (Krom and Berner, 1980) or precipitation of PO_4^{3-}–$CaCO_3$ complexes (Coelho et al., 2002) are possible sinks that were not quantified in this experiment.

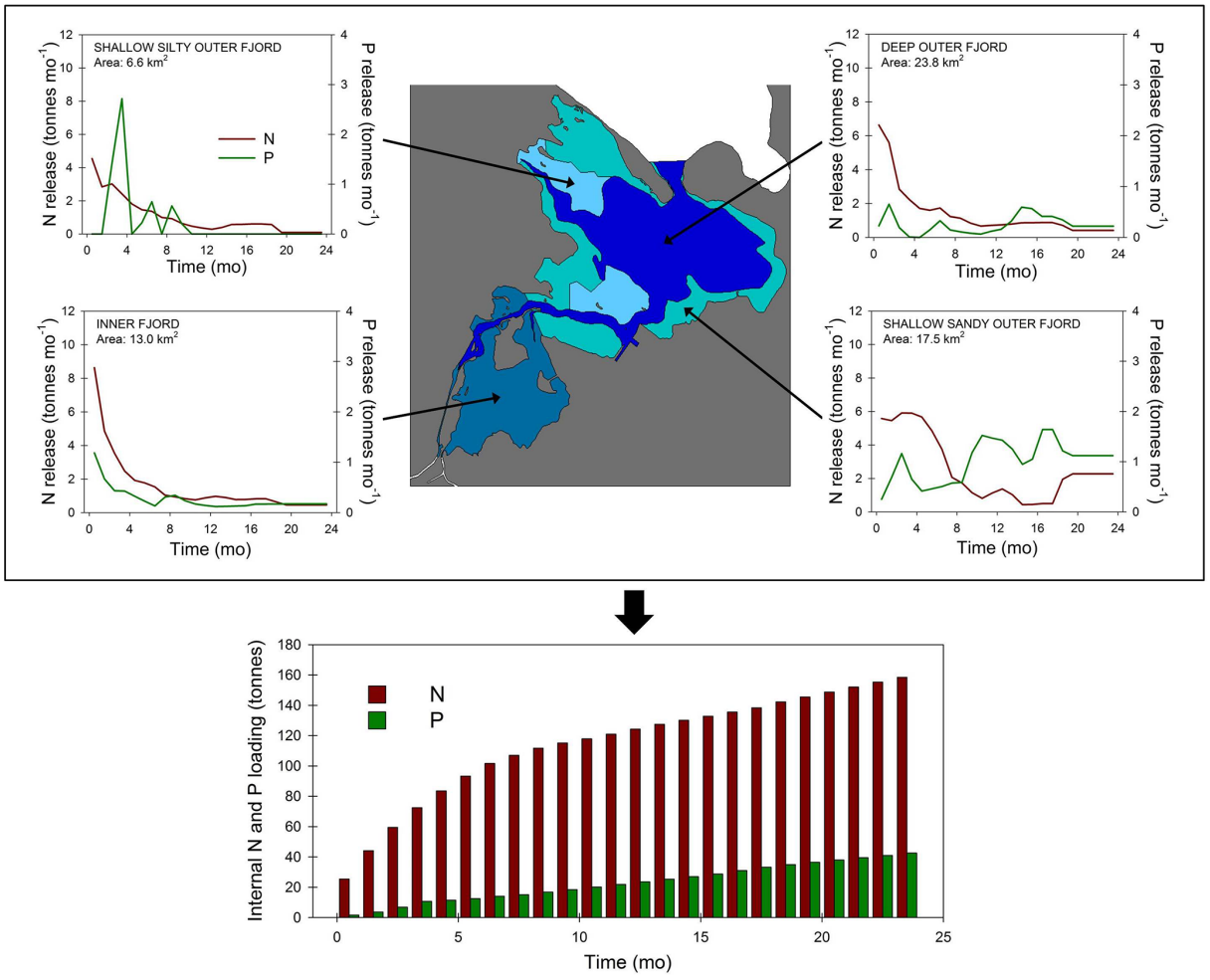

Figure 6. Estimated internal nutrient loading in Odense Fjord. The upper figure shows a schematic overview of Odense Fjord with the distribution of sediment types included in this study and their nutrient release over a 24-month period. The lower figure shows the cumulated nutrient release from the entire fjord bottom.

4.4 Internal nutrient loading

We calculated the potential internal nutrient loading in Odense Fjord resulting from microbial mineralization of ON and OP for a 2-year period based on the measured nutrient effluxes. Average nutrient fluxes were calculated for each sediment type, i.e., shallow inner fjord (St 1–3), shallow silty outer fjord (St 4), sandy outer fjord (St 5) and deep outer fjord (St 6–8). The monthly time-weighted DIN and PO_4^{3-} fluxes and the total areal distribution of the different sediment types in Odense Fjord were then used to calculate the total internal nutrient loading (10^3 kg N and P mo^{-1}) for each sediment type and for the whole ecosystem. Evidently these calculations do not represent the in situ internal nutrient loading, since effects of the otherwise continuous deposition of organic matter were omitted in the experimental setup. It can also be debated whether all the released nutrients can be considered internal nutrient loading, since the mineralization of recently deposited organic matter in surface sediments drove the majority of nutrient release during the first ~200 days. This nutrient release is largely determined by the ecosystem primary productivity extending only a few years back, and is therefore closely coupled to the recent levels of external nutrient loading. In any case the calculations represent the nutrient release resulting from the mineralization of slowly reacting ON and OP which have accumulated in the sediments.

The calculations show the magnitude of nutrient release driven by microbial mineralization of sediment-bound ON and OP in eutrophic ecosystems (Fig. 6). Total DIN release from the whole fjord bottom is equivalent to 121×10^3 kg N yr^{-1} (~ 20 kg N ha^{-1} yr^{-1}) the first year after sedimentation of new organic matter has ceased, but only 38×10^3 kg N yr^{-1} (~ 6.2 kg N ha^{-1} yr^{-1}) the second year, since ON effluxes decreased exponentially at all stations. The shallow sandy sediments in the outer fjord were most im-

portant for the total fjord-wide N release (39 %), whereas the remaining three sediment types contributed equally (16–23 %). The numbers for internal N loading are impressive at first, but they only correspond to maximum 2–6 % (N) of the current external N loading to Odense Fjord (about 2000×10^3 kg N yr^{-1}; Petersen et al., 2009). In the shallow N-limited Odense Fjord the internal N loading can therefore only have minor effects on overall ecosystem productivity. In any case the external N loading is far more important for the overall primary productivity and ecological status.

The internal P loading showed different temporal dynamics than internal N loading. Total P release from the whole fjord bottom was stable over time at rates of 21–22×10^3 kg P yr^{-1} ($\sim$ 3.4–3.6 kg P ha^{-1} y^{-1}; Fig. 6), while internal N loading decreased exponentially. The stability was driven by the increasing P release in shallow sandy outer fjord sediment and constant P release in deep outer fjord sediment. As for N, the shallow sandy sediments in the outer fjord was most important for total internal P loading (57 %) and the remaining three sediment types contributed equally (14–15 %). The internal P loading corresponded to 35–36 % (P) of the current external P loading to Odense Fjord (60×10^3 kg P yr^{-1}; Petersen et al., 2009) and thus potentially constitutes a stable and significant P source in the system. However, since Odense Fjord and most other temperate coastal ecosystems are mostly N-limited (Howarth et al., 2011), it is uncertain to which degree this excess P will affect ecosystem productivity.

4.5 Ecological implications

In many shallow eutrophic estuaries the external nutrient loading has been reduced to induce oligotrophication, but lower nutrient concentrations in the recipient estuary often occur after considerable delay and rarely correspond proportionally to the reductions (Kronvang et al., 2005; Carstensen et al., 2006). This indicates that a transient phase occurs, where accumulated nutrients are being released from the soils and sediments in the water shed and receiving estuary, respectively, while the system equilibrates to a new level of external nutrient loading. Our study shows the magnitude and temporal dynamics of the internal nutrient loading that can be expected in shallow estuaries recovering from eutrophication. It appears that internal N loading will be insignificant during recovery since it only corresponded to 2–6 % of the external N loading in our example and decreased rapidly. Internal N loading will therefore only lead to marginally elevated N availability and have minor effects on primary productivity and eutrophication status. The results are different with respect to PO_4^{3-}, since the internal P loading was stable and corresponded to $> 1/3$ of the external P loading. Internal P loading may therefore be a significant source of dissolved PO_4^{3-} for extended time in shallow eutrophic estuaries, and at a sufficiently high level to counteract reductions in the external P loading. Most shallow estuaries are N-limited (Conley et al., 2002; Howarth and Marinho, 2006; Howarth et al., 2011), so a high internal P loading might only exacerbate N limitation while having no further consequences for ecological quality. Decreasing internal N loading and stable internal P loading could also lead to increased dominance of cyanobacteria, which have low requirements for dissolved N. However, major shifts in phytoplankton communities would only occur in systems where decreased internal nutrient loading results in markedly lower DIN concentrations in the water phase, i.e., in systems where N loading is low and internal nutrient sources dominate.

The estimates of internal nutrient loading presented here provide an illustrative example, but the exact values are only valid for the experimental conditions and must be extrapolated with caution. Microbial reaction rates and DIN and PO_4^{3-} release from sediments are strongly influenced by ambient conditions. For instance, sediment macrofauna may stimulate the rates of organic matter degradation and sediment nutrient release through bioturbation (e.g., Kristensen et al., 2012, 2014), leading to higher internal nutrient loading than estimated from defaunated sediment cores in this experiment. Similarly, microbial mineralization processes and hence sediment DIN and PO_4^{3-} release are strongly temperature-dependent (Westrich and Berner, 1988; Sanz-Lazaro et al., 2011) and the magnitude of internal nutrient loading will therefore vary seasonally compared to our estimates based on a constant temperature experiment. Finally, in our experimental setup we also omitted hydrodynamics and porewater advection, which are known to stimulate nutrient cycling in shallow permeable sediments (Cook et al., 2007; Huettel et al., 2014). This will especially affect the estimated nutrient release from the sandy sediments from this study. Given the multitude of factors influencing nutrient mineralization rates, the actual magnitude of internal nutrient loading and related consequences for primary productivity will therefore follow a seasonal pattern driven by, for example, temperature, hydrodynamics, and composition and activity of benthic fauna. Other environmental variables such as hypoxia in the water column may also influence the magnitude of internal nutrient loading, since it hampers PO_4^{3-} retention by iron oxides (Azzoni et al., 2005; Mort et al., 2010; Viktorsson et al., 2013) and limits coupled nitrification–denitrification while stimulating dissimilatory nitrate reduction to NH_4^+ (Christensen et al., 2000; Jäntti and Hietanen, 2012). Ecosystems suffering from hypoxia may therefore experience a much higher internal nutrient loading than measured in this experiment. A comparison between total ON and OP mineralization and effluxes from this experiment suggests that nutrient effluxes could potentially increase 3–6-fold (DIN) and 2–10-fold (PO_4^{3-}) if there are no mechanisms to transform or retain inorganic nutrients at the sediment surface.

5 Conclusions

In this study we investigated the mineralization of organic N and P buried in the sediments from a shallow eutrophic estuary and obtained estimates of the magnitude and temporal dynamics of internal nutrient loading. Total internal N loading, which attenuated rapidly, corresponded to only a minor fraction of the external N loading and was therefore not important for the ecological state in the studied ecosystem. Total internal P loading showed no temporal attenuation and was quantitatively more important as it corresponded to more than one-third of the external P loading. However, the studied ecosystem was N-limited, and it is therefore uncertain whether high internal P loading will result in negative ecological effects. This study indicates that internal nutrient loading, and especially internal N loading, is a transient phenomena that can only temporarily influence the recovery trajectory of ecosystems recovering from eutrophication. In turn, internal nutrient loading driven by mineralization of organic N and P in sediments cannot explain the lack of recovery in shallow estuaries where external nutrient loading has been reduced.

Acknowledgements. The authors thank the people who helped with sampling, experimental work or analysis during this experiment (the crew aboard *Liv II*, Birthe Christensen, Rikke Orloff Holm, Maria Del Mar Sánchez Huertas and Maria Jensen). This project was funded by the Danish Strategic Science Foundation through grant 09-063190/DSF. C. O. Quintana was funded by FAPESP (São Paulo Research Support Foundation) grant # 2012/06121-1.

Edited by: C. P. Slomp

References

Aller, R. C. and Yingst, J. Y: Relationships between microbial distributions and the anaerobic decomposition of organic-matter in surface sediments of Long-Island Sound, USA, Mar. Biol., 56, 29–42, 1980.

Azzoni, R., Gianmarco, G., and Viaroli, P.: Iron-sulphur-phosphorous interactions: implications for sediment buffering capacity in a mediterranean eutrophic lagoon, Hydrobiologia, 550, 131–148, 2005.

Bower, C. E. and Holm-Hansen, T.: A salicylate-hypochlorite method for determining ammonia in seawater, Can. J. Fish. Aquat. Sci., 37, 794–798, 1980.

Boynton, W. R. and Kemp, W. M.: Nutrient regeneration and oxygen-consumption by sediments along an estuarine gradient, Mar. Ecol.-Prog. Ser., 23, 45–55, 1985.

Bukaveckas, P. A. and Isenberg, W. N.: Loading, transformation, and retention of Nitrogen and Phosphorus in the tidal freshwater James River (Virginia), Estuar. Coast., 36, 1219–1236, 2013.

Burdige, D. J.: The kinetics of organic-matter mineralization in anoxic marine sediments, J. Mar. Res., 49, 727–761, 1991.

Burgin, A. J. and Hamilton, S. K.: Have we overemphasized the role of denitrification in aquatic ecosystems?, A review of nitrate removal pathways, Front. Ecol. Environ., 5, 89–96, 2007.

Carstensen, J., Conley, D. J., Andersen, J. H., and Aertebjerg, G.: Coastal eutrophication and trend reversal: A Danish case study, Limnol. Oceanogr., 51, 398–408, 2006.

Christensen, P. B., Rysgaard, S., Sloth, N. P., Dalsgaard, T., and Schwærter, S.: Sediment mineralization, nutrient fluxes, denitrification and dissimilatory nitrate reduction to ammonium in an estuarine fjord with sea cage trout farms., Aquat. Microb. Ecol., 21, 73–84, 2000.

Coelho, J. P., Flindt, M. R., Jensen, H. S., Lillebo, A. I., and Pardal, M. A.: Phosphorus speciation and availability in intertidal sediments of a temperate estuary: relation to eutrophication and annual P-fluxes, Estuar. Coast. Shelf S., 61, 583–590, 2004.

Conley D. J., Markager, S., Andersen, J., Ellermann, T., and Svendsen L. M.: Coastal eutrophication and the Danish National Aquatic Monitoring and Assessment Program, Estuaries, 25, 848–861, 2002.

Cook, P. L. M., Wenzhofer, F., Glud, R. N., Janssen, F., and Huettel, M.: Benthic solute exchange and carbon mineralization in two shallow subtidal sandy sediments: Effect of advective pore-water exchange, Limnol. Oceanogr., 52, 1943–1963, 2007.

Cowan, J. L. W. and Boynton, W. R.: Sediment-water oxygen and nutrient exchanges along the longitudinal axis of Chesapeake Bay: Seasonal patterns, controlling factors and ecological significance, Estuaries, 19, 562–580, 1996.

Fulweiler, R. W., Nixon, S. W., and Buckley, B. A.: Spatial and temporal variability of benthic oxygen demand and nutrient regeneration in an anthropogenically impacted New England Estuary, Estuar. Coast., 33, 1377–1390, 2010.

Fyns Amt: Miljøfarlige stoffer og ålegræs i Odense Fjord, Fyns Amt, Natur-og Vandmiljøafdelingen, Odense, 1–108, 2006.

Gunnars, A. and Blomqvist, S.: Phosphate exchange across the sediment–water interface when shifting from anoxic to oxic conditions – an experimental comparison of freshwater and brackish-marine systems, Biogeochemistry, 37, 203–226, 1997.

Holmboe, N. and Kristensen, E.: Ammonium adsorption in sediments of a tropical mangrove forest (Thailand) and a temperate Wadden Sea area (Denmark), Wetl. Ecol. Manag., 10, 453–460, 2002.

Howarth, R. W. and Marino, R.: Nitrogen as the limiting nutrient for eutrophication in coastal marine ecosystems: evolving views over three decades, Limnol. Oceanogr., 51, 364–376, 2006.

Howarth, R., Chan, F., Conley, D. J., Garnier, J., Doney, S. C., Marino, R., and Billen, G.: Coupled biogeochemical cycles: eutrophication and hypoxia in temperate estuaries and coastal marine ecosystems, Front. Ecol. Environ., 9, 18–26, 2011.

Huettel, M., Berg, P., and Kostka, J. E.: Benthic Exchange and Biogeochemical Cycling in Permeable Sediments, Ann. Rev. Mar. Sci., 6, 23–51, 2014.

Hulth, S., Aller, R. C., Canfield, D. E., Dalsgaard, T., Engström, P., Gilbert, F., Sundbäck, K., and Thamdrup, B.: Nitrogen removal in marine environments: recent findings and future research challenges, Mar. Chem., 94, 125–145, 2005.

Hulthe, G., Hulth, S., and Hall P. O. J.: Effect of oxygen on degradation rate of refractory and labile organic matter in continental margin sediments, Geochim. Cosmochim. Ac., 62, 1319–1328, 1998.

Jantti, H. and Hietanen, S.: The effects of hypoxia on sediment nitrogen cycling in the Baltic Sea, Ambio, 41, 161–169, 2012.

Jensen, H. S., Mortensen, P. B., Andersen, F. O., Rasmussen, E., and Jensen, A.: Phosphorous cycling in a coastal marine sediment, Aarhus Bay, Denmark, Limnol. Oceanogr., 40, 908–917, 1995.

Kelly, J. R. and Nixon, S. W.: Experimental studies of the effect of organic deposition on the metabolism of a coastal marine bottom community, Mar. Ecol.-Prog. Ser., 17, 157–169, 1984.

Koroleff, F.: Determination of phosphorus, in: Method of Seawater Analysis, edited by: Grashof, K., Erhardt, M., and Kremling, K., Verlag Chemie, Weinheim, 125–131, 1983.

Kristensen, E. and Hansen, K.: Decay of plant detritus in organic-poor marine sediment: production rates and stoichiometry of dissolved C and N compounds, J. Mar. Res., 53, 675–702, 1995.

Kristensen, E., Mangion, P., Tang, M., Flindt, M. R., Holmer, M., and Ulomi, S.: Microbial carbon oxidation rates and pathways in sediments of two Tanzanian mangrove forests, Biogeochemistry, 103, 143–58, 2011.

Kristensen, E., Penha-Lopes, G., Delefosse, M., Valdemarsen, T., Quintana, C., and Banta, G.: What is bioturbation? The need for a precise definition for fauna in aquatic sciences, Mar. Ecol.-Prog. Ser., 446, 285–302, 2012.

Kristensen, E., Delefosse, M., Quintana, C. O., Flindt, M. R., and Valdemarsen, T.: Influence of benthic macrofauna on ecosystem functioning in a shallow Danish estuary, Front. Mar. Sci., 1, 41, doi:10.3389/fmars.2014.00041, 2014.

Krom, M. D. and Berner, R. A.: Adsorbtion of phosfate in anoxic marine sediments, Limnol. Oceanogr., 25, 797–806, 1980.

Kronvang, B., Jeppesen, E., Conley, D. J., Sondergaard, M., Larsen, S. E., Ovesen, N. B., and Carstensen, J.: Nutrient pressures and ecological responses to nutrient loading reductions in Danish streams, lakes and coastal waters, J. Hydrol., 304, 274–288, 2005.

Lomstein, B. A., Jensen, A. G. U., Hansen, J. W., Andreasen, J. B., Hansen, L. S., Berntsen, J., and Kunzendorf, H.: Budgets of sediment nitrogen and carbon cycling in the shallow water of Knebel Vig, Denmark, Aquat. Microb. Ecol., 14, 69–80, 1998.

Lovley, D. R. and Phillips, E. J. P.: Rapid assay for microbially reducible ferric iron in aquatic sediments, Appl. Environ. Microb., 53, 1536–1540, 1987.

Mackin, J. E. and Aller, R. C.: Ammonium adsorption in marine sediments, Limnol. Oceanogr., 29, 250–257, 1984.

Mackin, J. E. and Swider, K. T.: Organic matter decomposition pathways and oxygen consumption in coastal marine sediments, J. Mar. Res., 47, 681–716, 1989.

Mort, H. P., Slomp, C. P., Gustafsson, B. G., and Andersen, T. J.: Phosphorus recycling and burial in Baltic Sea sediments with contrasting redox conditions, Geochim. Cosmochim. Ac., 74, 1350–1362, 2010.

Mortazavi, B., Riggs, A. A., Caffrey, J. M., Genet, H., and Phipps, S. W.: The contribution of benthic nutrient regeneration to primary production in a shallow eutrophic estuary, Weeks Bay, Alabama, Estuar. Coast., 35, 862–877, 2012.

Nielsen, K. P. L. and Rasmussen, P.: Estuarine nitrogen retention independently estimated by the denitrification rate and mass balance methods: a study of Norsminde Fjord, Denmark, Mar. Ecol.-Prog. Ser., 119, 275–283, 1995.

Petersen, J. D., Rask, N., Madsen, H. B., Jorgensen, O. T., Petersen, S. E., Nielsen, S. V. K., Pedersen, C. B., and Jensen, M. H.: Odense Pilot River Basin: implementation of the EU Water Framework Directive in a shallow eutrophic estuary (Odense Fjord, Denmark) and its upstream catchment, Hydrobiologia, 629, 71–89, 2009.

Pitkanen, H., Lehtoranta, J., and Raike, A.: Internal nutrient fluxes counteract decreases in external load: the case of the estuarial eastern Gulf of Finland, Baltic Sea, Ambio, 30, 195–201, 2001.

Quintana, C., Kristensen, E., and Valdemarsen, T.: Impact of the invasive polychaete Marenzelleria viridis on the biogeochemistry of sandy marine sediments, Biogeochemistry, 115, 95–109, 2013.

Riisgard, H. U. and Banta, G. T.: Irrigation and deposit feeding by the lugworm Arenicola marina, characteristics and secondary effects on the environment, A review of current knowledge, Vie Milieu – Life and Environment, 48, 243–257, 1998.

Rozan, T. F., Taillefert, M., Trouwborst, R. E., Glazer, B. T., Ma, S. F., Herszage, J., Valdes, L. M., Price, K. S., and Luther, G. W.: Iron-sulfur-phosphorus cycling in the sediments of a shallow coastal bay: implications for sediment nutrient release and benthic macroalgal blooms, Limnol. Oceanogr., 47, 1346–1354, 2002.

Sanz-Lazaro, C., Valdemarsen, T., Marin, A., Holmer, M., Effect of temperature on biogeochemistry of marine organic-enriched systems: implications in a global warming scenario, Ecol. Appl., 21, 2664–2677, 2011.

Seitzinger, S. P.: Denitrification in fresh-water and coastal marine ecosystems – ecological and geochemical significance, Limnol. Oceanogr., 33, 702–724, 1988.

Stookey, L. L.: Ferrozine – a new spectrophotometric reagent for iron, Anal. Chem., 42, 779–781, 1970.

Sundby, B., Gobeil, C., Silverberg, N., and Mucci, A.: The phosphorous cycle in coastal marine sediments, Limnol. Oceanogr., 37, 1129–1145, 1992.

Tobias, C., Giblin, A., McClelland, J., Tucker, J., and Peterson, B.: Sediment DIN fluxes and preferential recycling of benthic microalgal nitrogen in a shallow macrotidal estuary, Mar. Ecol.-Prog. Ser., 257, 25–36, 2003.

Tyler, A. C., McGlathery, K. J., and Anderson, I. C.: Benthic algae control sediment-water column fluxes of organic and inorganic nitrogen compounds in a temperate lagoon, Limnol. Oceanogr., 48, 2125–2137, 2003.

Valdemarsen, T. and Kristensen, E.: Diffusion scale dependent change in anaerobic carbon and nitrogen mineralization: true effect or experimental artifact?, J. Mar. Res., 63, 645–669, 2005.

Valdemarsen, T., Kristensen, E., and Holmer, M.: Metabolic threshold and sulfide-buffering in diffusion controlled marine sediments impacted by continuous organic enrichment, Biogeochemistry, 95, 335–353, 2009.

Valdemarsen, T., Canal-Verges, P., Kristensen, E., Holmer, M., Kristiansen, M. D., and Flindt, M. R.: Vulnerability of Zostera marina seedlings to physical stress, Mar. Ecol.-Prog. Ser., 418, 119–130, 2010.

Valdemarsen, T., Wendelboe, K., Egelund, J. T., Kristensen, E., and Flindt, M. R.: Burial of seeds and seedlings by the lugworm Arenicola marina hampers eelgrass (Zostera marina) recovery, J. Exp. Mar. Biol. Ecol., 410, 45–52, 2011.

Valdemarsen, T., Bannister, R. J., Hansen, P. K., Holmer, M., and Ervik, A.: Biogeochemical malfunctioning in sediments beneath a deep-water fish farm, Environ. Pollut., 170, 15–25, 2012.

Valdemarsen, T., Quintana, C. O., Kristensen, E., and Flindt, M. R.: Recovery of organic enriched sediments through microbial degradation - implications for eutrophic estuaries, Mar. Ecol.-Prog. Ser., 503, 41–58, 2014.

Viktorsson, L., Ekeroth, N., Nilsson, M., Kononets, M., and Hall, P. O. J.: Phosphorus recycling in sediments of the central Baltic Sea, Biogeosciences, 10, 3901–3916, doi:10.5194/bg-10-3901-2013, 2013.

Wendelboe, K., Egelund, J. T., Flindt, M. R., and Valdemarsen, T.: Impact of lugworms (Arenicola marina) on mobilization and transport of fine particles and organic matter in marine sediments, J. Sea Res., 76, 31–38, 2013.

Westrich, J. T. and Berner, R. A.: The role of sedimentary organic matter in bacterial sulfate reduction: the G-model tested, Limnol. Oceanogr., 29, 236–249, 1984.

Westrich, J. T. and Berner, R. A., The effect of temperature on rates of sulfate reduction in marine sediments, Geomicrobiol. J., 6, 99–117, 1988.